Nanoscale Research Letters

NANO EXPRESS Open Access

Recyclable and Flexible Starch-Ag Networks and Its Application in Joint Sensor

Sai Liu[1†], Cong Chen[1†], Dongwei Zhang[1], Guanping Dong[1,2], Dongfeng Zheng[1], Yue Jiang[1*], Guofu Zhou[3], Jun-Ming Liu[4], Krzysztof Kempa[5] and Jinwei Gao[1*]

Abstract

Flexible transparent conductive electrodes are essential component for flexible optoelectronic devices and have been extensively studied in recent years, while most of the researches are focusing on the electrode itself, few topics in material green and recyclability. In this paper, we demonstrate a high-performance transparent conductive electrode (TCE), based on our previous cracking technology, combined with a green and recyclable substrate, a starch film. It not only shows low R_s (less than 1.0 Ω sq^{-1}), high transparency (> 82%, figure of merit ≈ 10,000), but also provides an ultra-smooth morphology and recyclability. Furthermore, a series of biosensors on human joints are demonstrated, showing great sensitivity and mechanical stability.

Keywords: Starch-ANs, Recyclability, Optoelectronics, Ultra-smooth morphology, Sensor

Introduction

Currently, electronic devices have been experiencing many new challenges, such as compatibility, mechanical flexibility, and eco-friendly manner [1–5]. Among those, transparent conductive electrode (TCE) as an important component of those devices is also facing new challenges, like high optical transmittance, low resistance, flexibility, biocompatibility [6], low-cost [7], and the recyclability [8]. Currently, indium tin oxide (ITO) [9] is the widely used TCE, which is a continuous and chemically stable film. However, its fragility induced by the metal oxide and the large expense because of rare metal highly limit its future development. On the other hand, graphene/metal grid [10, 11], for example, metal networks [12, 13] and metal nanowires [14–19], is facing serious adhesiveness and roughness problems. In addition, their high synthesizing cost and the impossibility to recycle make them detained in the laboratory.

In comparison, a series of TCEs based on crack-nanonetwork (CNN) [20] have been invented by our group, which presenting brilliant optoelectronic properties, high figure of merit, and the flexibility. With electroplating technology [21], we further realized the fully wet fabricated CNN based on UV glue with ultra-low sheet resistance (0.13 Ω sq^{-1}) and smooth morphology [22]. Currently, all of the substrates are based on the intrinsic non-degradation polymers, restraining the recycling of precious metal, like Ag and Au. Starch film is a transparent and flexible substrate material, and more importantly, it is an eco-friendly material and could be degraded in water. Jeong et al. [23] added PVA into a starch film and fabricated a flexible and disposable TCE; thus, it shows great potential of starch film as substrates.

Herein, we took the advantage of water degradability of starch film [24, 25] and fabricated a recyclable TCE, starch-Ag networks (SANs), through embedding our previously reported crack Ag networks in starch film. Via electroplating, we decreased the sheet resistance (R_s) to less than 1.0 Ω sq^{-1} along with highly optical transparency (> 82%) and high figure of merit (F) of over 10,000. Moreover, due to the peeling off fabrication process and self-supporting network [26], SAN presents good flexibility, low surface roughness, and the recyclability. Besides, SAN was used to demonstrate its application in biosensors in human joint with good sensitivity and mechanical stability.

* Correspondence: yuejiang@m.scnu.edu.cn; gaojw@scnu.edu.cn
Sai Liu and Cong Chen are equal contributors.
†Sai Liu and Cong Chen contributed equally to this work.
[1]Institute for Advanced Materials, South China Academy of Advanced Optoelectronics, South China Normal University, Guangzhou 510006, China
Full list of author information is available at the end of the article

Methods

Fabrication Process

Figure 1a schematically presents the fabrication process of the SANs. Step 1 is to prepare the network template with the method invented by our group [27]. Firstly, the egg white self-cracks during drying process thereby form the channel networks. After the deposition of Ag seed layer with sputtering (step 2), the sacrificial layer is washed away. Subsequently, a dense layer of Ag is further deposited on the surface of seed layer metal network via electroplating deposition (step 3). In step 4, the Ag networks are covered with starch film by dip coating the prepared starch solution and drying naturally. Finally, the Ag networks embedded in starch are peeled off from quartz. On account that the gelatinization temperature of normal starch is intrinsically high (usually more than 90 °C) [28], herein starch mechanical property is enhanced by its room temperature gelatinization.

Preparation of the Sacrificial Template

Self-cracking materials are a mixture of egg white and deionized water (3:1 by volume). A cracking template is obtained by dip coating above solution on a glass (50 mm × 50 mm), then drying in air about 10 mins, and finally, the self-cracking process occurs.

Ag Seed Layer Deposition

Sputtering (AJA International ATC Orion 8, USA) was used to deposit Ag seed layers (≈ 60 nm) on self-cracking template. Then, the sacrificial layer is removed by rinsing in deionized water.

Electroplating of Ag Networks Based on CNN Layers

One hundred-milliliter Ag electroplate liquid composed of 4 g $AgNO_3$, 22.5 g $Na_2S_2O_3{\cdot}5H_2O$, and 4 g $KHSO_3$ in deionized water was used for the electroplating deposition. A homemade plating bath is used in the process,

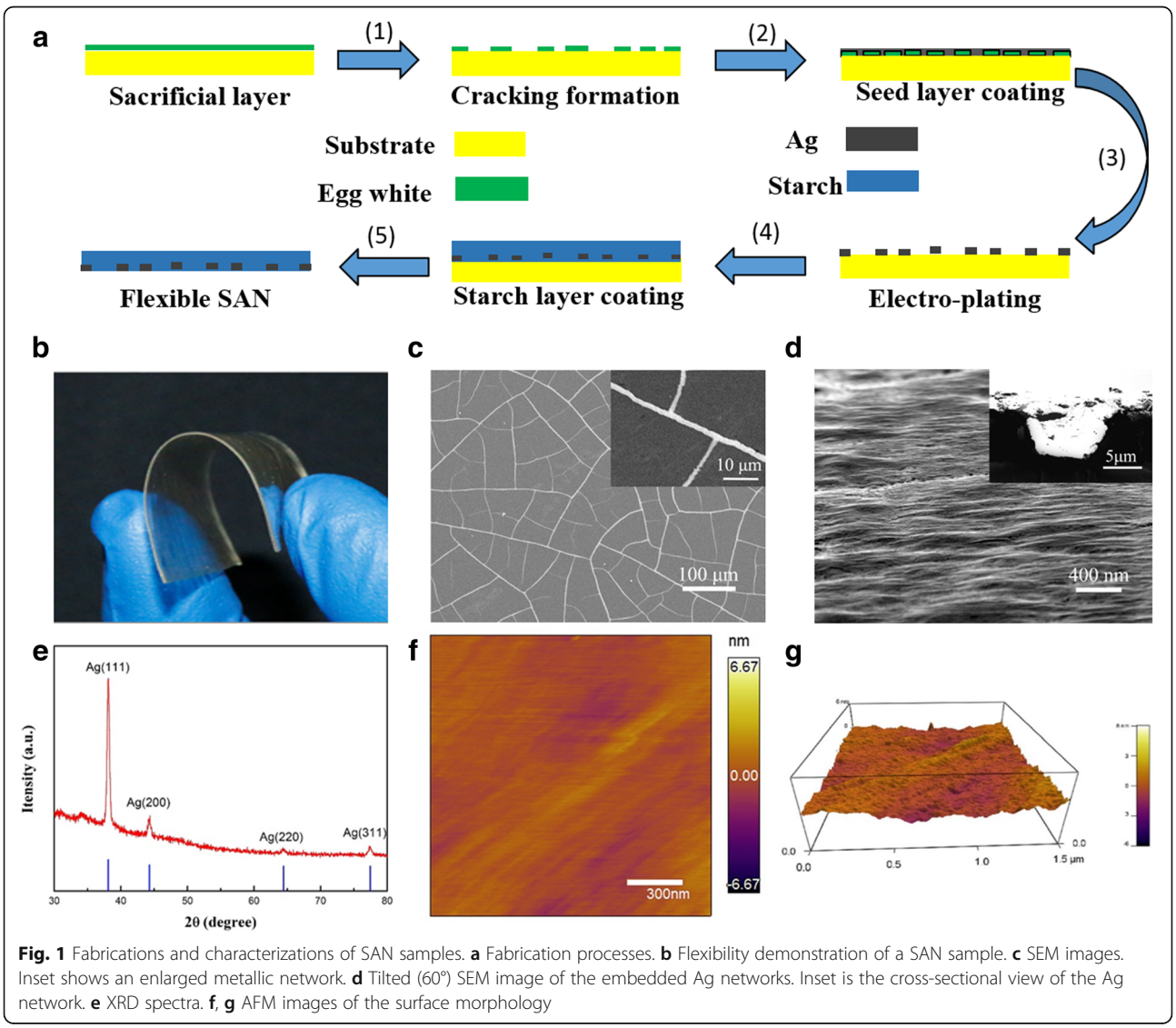

Fig. 1 Fabrications and characterizations of SAN samples. **a** Fabrication processes. **b** Flexibility demonstration of a SAN sample. **c** SEM images. Inset shows an enlarged metallic network. **d** Tilted (60°) SEM image of the embedded Ag networks. Inset is the cross-sectional view of the Ag network. **e** XRD spectra. **f**, **g** AFM images of the surface morphology

with a seed layer as the cathode and a Ag bar (40 mm × 40 mm) as the anode. The current for the electroplating deposition is 10 mA. We changed the thickness of the film by controlling the plating time. Finally, the Ag networks were rinsed in deionized water.

Fabrication of a Starch TCE

The starch solution, composed of 12.5 g corn starch, 1.25 g glycerinum (10 wt%) in 100 ml deionized water, was prepared at 60 °C on a hot plate, with stirring at 500 rpm for 30 min. The bubbles were removed from the starch solution in vacuum environment for 2 h. Four-milliliter starch solution was dip coated on the electroplating TCE and then dried in air for about 20 h under 30–40% RH and 25 °C.

Transfer of Ag Networks

The starch-Ag network film was immersed in DI water under 25 °C for 2 h. Then, the starch layer is dissolved, and finally, the freestanding Ag network was obtained.

Characterizations

The morphologies of samples were conducted by a SEM (ZEISS Gemini 500, Garl Zeiss, Germany), photographic camera, and atomic force microscope (AFM) (Cypher, Asylum Research). The crystallinity and phase information of the metal particles were determined by an X-ray diffraction system (PAN analytical X'Pert-Pro MPD PW 3040/60 XRD with Cu-Kα1 radiation, Netherlands). Optical transmittance was measured using an integrating sphere system (Ocean Optics, USA). Sheet resistance of samples was measured by a van der Pauw method, with four silver paste contacts deposited at the corners of a square sample (20 mm × 20 mm), recording with a Keithley 2400 SourceMeter (Keithley, USA). Two-probe resistance method is conducted in a bending test (Additional file 1).

Results and Discussion

Sample Morphologies

Figure 1b is a schematic figure of the obtained SAN sample, showing a good flexibility and transparency. The SEM image of the metallic network is shown in Fig. 1c, with an average width and height of the Ag networks 2.5 μm and 1 μm respectively, and the inter-thread spacing in the range of 30 to 60 μm. The inset in Fig. 1c clearly displays the detailed morphology of the metal networks. The surface morphology of the SAN film is shown in Fig. 1d, with the inset of cross-sectional image, proving that the Ag networks have been successfully embedded into the starch film and exhibiting a smooth morphology. In addition, the height of Ag networks could be easily modulated by changing the concentration of the electroplating liquid, anode area, and distance between an anode and cathode in the electroplating deposition process [29], while the width of the networks and the inter-space can be controlled by varying the sacrificial material, concentration, and cracking temperature, as reported in our previous work [30]. The crystallinity of SAN was characterized by X-ray diffraction (XRD) (Fig. 1e), which exhibits the (200), (220), and (311) planes of Ag, and no impurity detected. Atomic force microscopy (AFM) images in Fig. 1f, g confirmed an ultra-smooth surface with an extremely low root-mean-square (RMS) roughness of ~ 0.521 nm.

Optical and Mechanical Performance

Figure 2a shows the transmittance (T) versus the sheet resistance (R_s) plots, comparing the optoelectronic properties of the SAN with other reported TCEs [5, 6, 31–

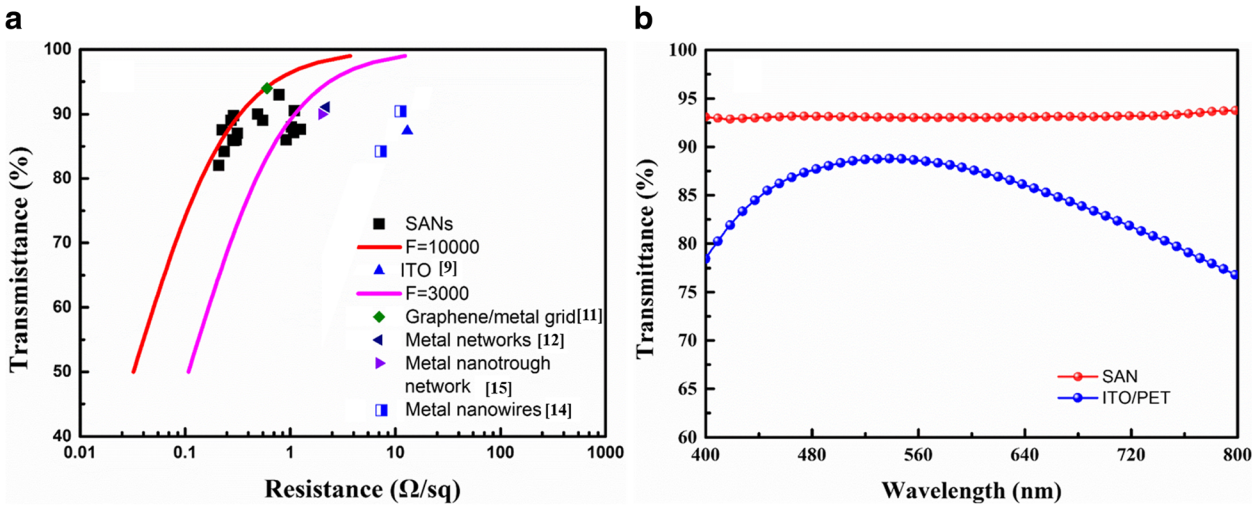

Fig. 2 Optoelectronic properties of the metallic networks. **a** Optical transmittance of metallic networks as a function of sheet resistance. **b** Transmittance versus wavelength of the SAN and a ITO/PET sample

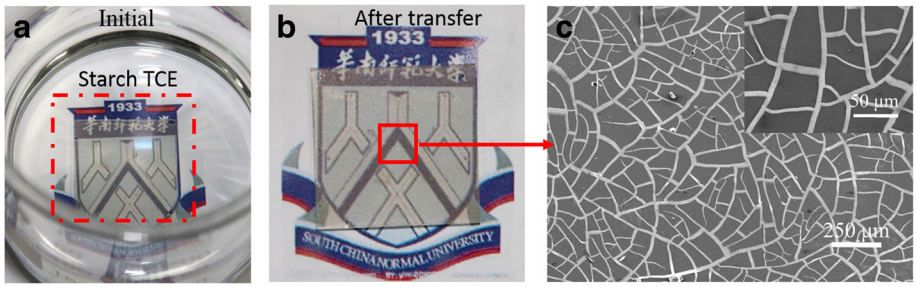

Fig. 3 Recyclability test of a SAN in water: **a** original and **b** after transfer. **c** SEM images of recycled Ag networks

36] and a commercial ITO film (150 nm thick, Liaoning Huite Photoelectric Technology). A figure of merit (*F*), shown as lines, is determined by fitting the equation in [37]. Our SAN shows very good optoelectronic properties with the high transparency (82–93%) and low sheet resistance (0.2–1.0 Ωsq^{-1}, with *F* ranging from 3000 to 10,000) based on different cracking templates [38]. These data are significantly better than those of conventional ITO and other grid TCEs, which could be ascribed to the excellent crystallinity of Ag, the continuous morphology, and the appropriate network structure. Figure 2b shows optical transmittance of the SAN and ITO/PET (150 nm thick, Liaoning Huite Photoelectric Technology Co., Ltd.). It is clear that the optical transmittance of the SAN (~ 93%) is much higher than that of ITO/PET (77~88%) in the entire visible spectrum.

Recyclable

Starch is not only a green material and non-toxic for human beings or the environment, but also a biodegradable material, as well as easily removed by water [39]. These properties, therefore, endow the SAN a recyclable material as illustrated in Fig. 3. A piece of used SAN film was immersed into the water (Fig. 3a), and 2 h later, most of the starch substrate was degraded, and water turned into opaque state. The obtained freestanding Ag networks was washed with water to remove residue starch and then transferred onto a piece of a ITO glass and dried in a drying box (Fig. 3b). Figure 3c shows SEM images of the recycled Ag networks. It is worth mentioning that the recycling process keeps the integrity of the Ag networks due to its self-supporting property, rendering the recyclability of the process and finally

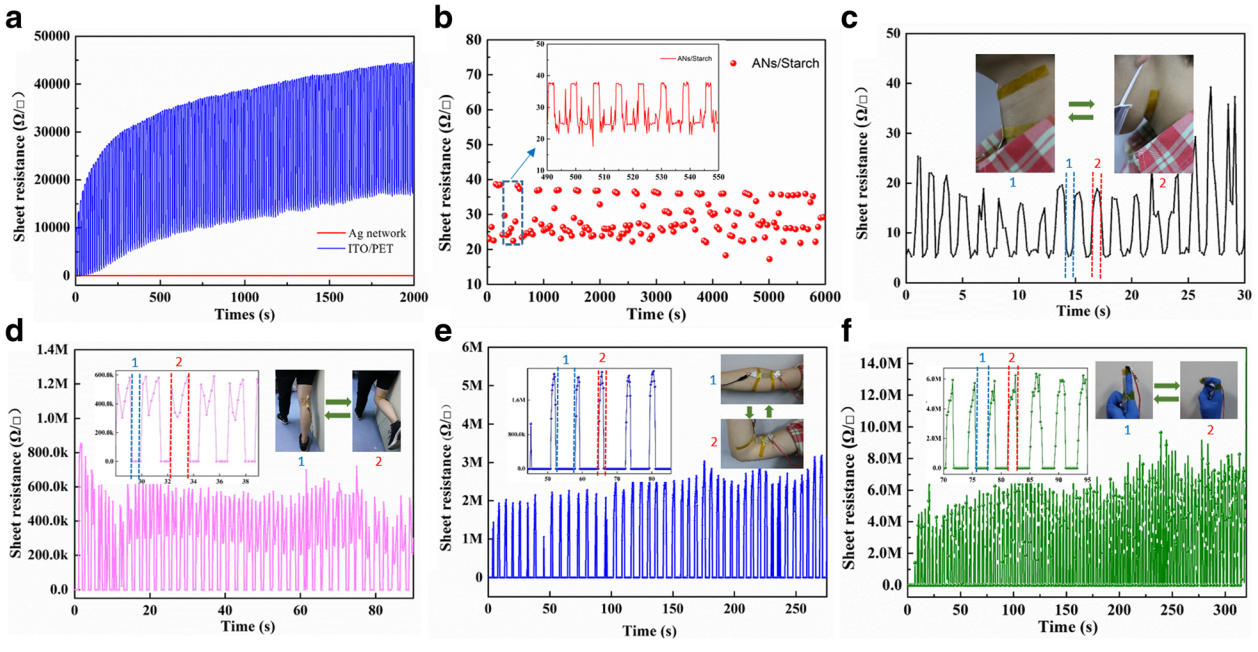

Fig. 4 Flexibility demonstration of the SAN based sensor. **a** Comparison of sheet resistance as a function of bending time. **b** An enlarged figure of **a**; inset shows the detailed variation of sheet resistance of the SAN sensor from 490 to 550 s. **c**–**f** Characterization of sensors bending at different part of human body: **c** neck, **d** knee, **e** elbow, and **f** finger. Insets: photographs of the sensors attached to different part of human body

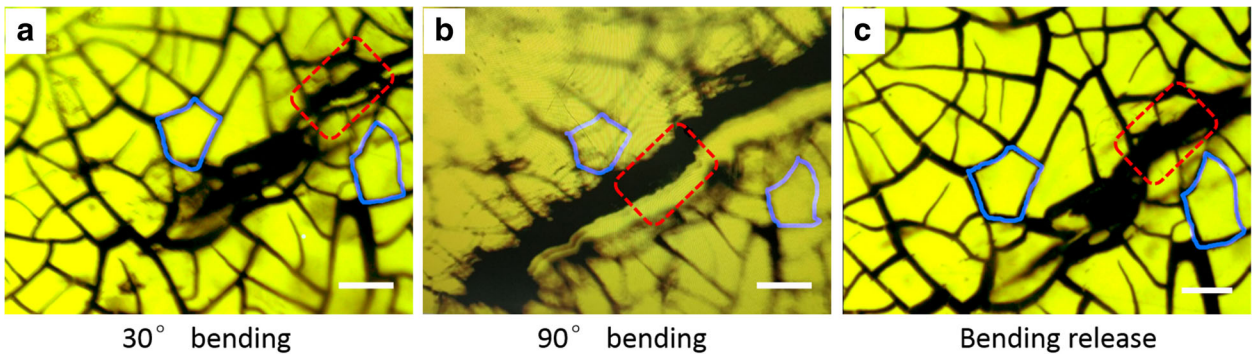

Fig. 5 Working mechanism of the SAN sensor at different stages: **a** 30° bending, **b** 90° bending, and **c** bending release. Scale bars in figures are 50 μm

reducing the overall cost and the environmental impact, comparing with the TCEs based on the non-degradable and non-recyclable plastic substrates [5, 9, 40–42].

Sensing Performance of the SAN

The flexibility of the SAN was characterized under bending in comparison with a ITO/PET sample. The R_s of ITO/PET raised significantly (~ 35,000 Ω sq^{-1}) within a thousand bending cycles (Fig. 4a), whereas the R_s of the SAN fluctuates around 30 Ω sq^{-1}, showing an excellent mechanical stability (Fig. 4a, b). Simultaneously, a periodic fluctuation of R_s was observed when the SAN was bent (from 24 to 38 Ω sq^{-1}) as shown in the inset of Fig. 4b, which is suggestive of its potential application on mechanical sensor [43–47]. Accordingly, a series of simple joint sensors were designed and fabricated [48–51]. The SAN with two narrow silver paste lines along edges to give better contact was sandwiched between two pieces of PET films, which was attached on the joint the of neck, knee, elbow, finger, respectively. The motion-dependent response of these sensors was recorded by a two-probe resistance measurement setup. When the joints were in bending stage, the R_s of the sensor changed correspondingly as demonstrated in Fig. 4c–f. When the SAN was under tensile stress at different parts of the body, the output signal varied in a wide range: on the neck, R_s is about 20–30 Ω sq^{-1} (Fig. 4c), on knee 400–800 KΩ sq^{-1}(Fig. 4d), on elbow 2–3 MΩ sq^{-1} (Fig. 4e), and on finger 4–8 MΩ sq^{-1} (Fig. 4f). These differences are possibly associated with the magnitude of movement and indicate that the performance of joint SAN sensor are location-dependent [52].

Figure 5 demonstrates the working mechanism of the SAN sensors, with blue lines locating the identical area. When the bending is limited to 30°, a subtle cracking was observed as indicated by the red rectangle in Fig. 5a. In spite of the difficulty to obtain a well-focused image, when the bending angle increased to 90°, the distance of this cracking slit was found further widened as well as its elongation (Fig. 5b). The re-flattening process, however, induced the recovery of the cracking which could barely be seen (Fig. 5c). In the meantime, the resistance of the SAN almost fully recovered to its initial state, as shown in Fig. 4a–d. Hence, the periodic variation of resistance during bending is attributed to the dynamic change of Ag network connection.

Conclusion

In conclusion, we have developed high-performance recyclable metallic networks, by combining the cracking network with starch substrates. The corresponding figure of merit of the resulting metallic network exceeds 10,000 with the sheet resistance (R_s) to less than 1.0 Ω sq^{-1} along with highly optical transparency (> 82%). Most importantly, the metallic network presents good flexibility, low surface roughness, and recyclability. Finally, a series of biosensors have been demonstrated showing good performance.

Additional file

Additional file 1: Figure S1. Images of SAN with different glycerin mass ratio. a) wt5%, b) wt10%, c) wt20%. **Figure S2.** (a) Photograph of the setup for bending test, which includes mobile station (1), controller of the mobile station (2, 3), voltage transformer (4), (5) Keithley 2400. (b) Schematic diagram of the bending test. **Table S1.** Comparison of sheet resistance as a recovering of time: original and after transfer. (DOCX 1585 kb)

Abbreviations

AFM: Atomic force microscopy; CNN: Crack-nanonetwork; *F*: Figure of merit; ITO: Indium tin oxide; RMS: Root-mean-square; R_s: Sheet resistance; SAN: Starch-Ag network; SEM: Scanning electron microscope; *T*: Transmittance; TCE: Transparent conductive electrode; XRD: X-ray diffraction

Acknowledgements

We thank the support from the Guangdong Provincial Engineering Technology Research Center for Transparent Conductive Materials, National Center for International Research on Green Optoelectronics (IrGO), MOE International Laboratory for Optical Information Technologies and the 111 Project.

Funding
We thank the financial support from NSFC-Guangdong Joint funding, China (No. U1801256), National Key R&D Program of China (No. 2016YFA0201002), Guangdong Provincial Foundation (2016KQNCX035), NSFC grant (No. 51803064, 51571094, 51431006, 51561135014, U1501244), Program for Chang Jiang Scholars and Innovative Research Teams in Universities (No. IRT_17R40) and Guangdong Innovative Research Team Program (No. 2013C102).

Availability of Data and Materials
All data can be provided on a suitable request.

Authors' Contributions
SL and JWG developed the idea. CC, ZDW, GPD, and ZDF prepared the samples and conducted the experiments. JWG, SL, and JY wrote the paper. All authors discussed the results and commented on the manuscript. JWG directed the research. All authors read and approved the final manuscript.

Competing Interests
The authors declare that they have no competing interests.

Publisher's Note

Author details
[1]Institute for Advanced Materials, South China Academy of Advanced Optoelectronics, South China Normal University, Guangzhou 510006, China. [2]School of Mechanical and Automotive Engineering, South China University of Technology, Guangzhou 510640, China. [3]Guangdong Provincial Key Laboratory of Optical Information Materials and Technology and Institute of Electronic Paper Displays, South China Academy of Advanced Optoelectronics, South China Normal University, Guangzhou 510006, China. [4]Laboratory of Solid State Microstructures, Nanjing University, Nanjing 210093, China. [5]Department of Physics, Boston College, Chestnut Hill, MA 02467, USA.

Received: 16 February 2019 Accepted: 25 March 2019
Published online: 05 April 2019

References

1. Li D, Lai W, Zhang Y, Huang W (2018) Printable transparent conductive films for flexible electronics. Adv Mater 30(10):1704738
2. Im H, An B, Jin J, Jang J, Park Y, Park J, Bae B (2016) A high-performance flexible and robust metal nanotrough-embedded transparent conducting film for wearable touch screen panels. Nanoscale 8(7):3916–3922
3. Wang S, Xu J, Wang W, Wang G, Rastak R, Molina-Lopez F, Lei T (2018) Skin electronics from scalable fabrication of an intrinsically stretchable transistor array. Nature 555(7694):83
4. Lipomi D, Vosgueritchian M, Tee B, Hellstrom S, Lee J, Fox C, Bao Z (2011) Skin-like pressure and strain sensors based on transparent elastic films of carbon nanotubes. Nat Nanotechnol 6(12):788
5. Pu J, Zha X, Tang L, Bai L, Bao R, Liu Z, Yang W (2018) Human skin-inspired electronic sensor skin with electromagnetic interference shielding for the sensation and protection of wearable electronics. ACS Appl Mater Interfaces 10(47):40880–40889
6. Lee D, Lim Y, Im H, Jeong S, Ji S, Kim Y, Bae B (2017) Bioinspired transparent laminated composite film for flexible green optoelectronics. ACS Appl. Mater. Interfaces 9(28):24161–24168
7. Zhong Z, Woo K, Kim I, Hwang H, Kwon S, Choi Y, Moon J (2016) Roll-to-roll-compatible flexible transparent electrodes based on self-nanoembedded Cu nanowires using intense pulsed light irradiation. Nanoscale 8(16):8995–9003
8. Lai J, Zhou H, Wang M, Chen Y, Jin Z, Li S,Yang J, Jin X, Liu Z, Zhao W (2018) Recyclable, stretchable and conductive double network hydrogels towards flexible strain sensors. J Mater Chem C 6(48):13316–13324.
9. Minami T (2008) Substitution of transparent conducting oxide thin films for indium tin oxide transparent electrode applications. Thin Solid Films 516(7): 1314–1321
10. Han B, Huang Y, Li R, Peng Q, Luo J, Pei K, Gao J (2014) Bio-inspired networks for optoelectronic applications. Nat Commun 5:5674
11. Gao T, Li Z, Huang P, Shenoy G, Parobek D, Tan S, Leu PW (2015) Hierarchical graphene/metal grid structures for stable flexible transparent conductors. ACS Nano 9(5):5440–5446
12. Peng Q, Pei K, Han B, Li R, Zhou G, Liu J, Gao J (2016) Inexpensive transparent nanoelectrode for crystalline silicon solar cells. Nanoscale Res Lett 11(1):312
13. Khan A, Lee S, Jang T, Xiong Z, Zhang C, Tang J, Li W (2016) High-performance flexible transparent electrode with an embedded metal mesh fabricated by cost-effective solution process. Small 12(22):3021–3030
14. Hsu P, Wang S, Wu H, Narasimhan V, Kong D, Lee H, Cui Y (2013) Performance enhancement of metal nanowire transparent conducting electrodes by mesoscale metal wires. Nat Commun 4:2522
15. Wu H, Kong D, Ruan Z, Hsu P, Wang S, Yu Z, Cui Y (2013) A transparent electrode based on a metal nanotrough network. Nat Nanotechnol 8(6):421
16. Kim T, Kim Y, Lee H, Kim H, Yang W, Suh K (2013) Uniformly interconnected silver-nanowire networks for transparent film heaters. Adv Funct Mater 23(10):1250–1255
17. Bao C, Yang J, Gao H, Li F, Yao Y, Yang B, Liu J (2015) In situ fabrication of highly conductive metal nanowire networks with high transmittance from deep-ultraviolet to near-infrared. ACS Nano 9(3):2502–2509
18. Manikandan A, Lee L, Wang YC, Chen CW, Chen YZ, Medina H, Tseng JY, Wang ZM, Chueh YL (2017) Graphene-coated copper nanowire networks as a highly stable transparent electrode in harsh environments toward efficient electrocatalytic hydrogen evolution reactions. J Mater Chem A 5(26):13320–13328
19. Tseng JY, Lee L, Huang YC, Chang JH, Su TY, Shih YC, Lin HW, Chueh YL (2018) Pressure welding of silver nanowires networks at room temperature as transparent electrodes for efficient organic light-emitting diodes. Small 14(38):1800541
20. Han B, Peng Q, Li R, Rong Q, Ding Y, Akinoglu E, Zhou G (2016) Optimization of hierarchical structure and nanoscale-enabled plasmonic refraction for window electrodes in photovoltaics. Nat Commun 7:12825
21. Liu A, Ren X, An M, Zhang J, Yang P, Wang B et al (2014) A combined theoretical and experimental study for silver electroplating. Sci Rep 4(5): 3837
22. Xian Z, Han B, Li S, Yang C, Wu S, Lu X, Naughton M (2017) A practical ITO replacement strategy: sputtering-free processing of a metallic nanonetwork. Adv Mater Tech 2(8):1700061
23. Jeong H, Baek S, Han S, Jang H, Kim S, Lee H (2018) Novel eco-friendly starch paper for use in flexible transparent and disposable organic electronics. Adv Funct Mater 28(3):1704433
24. Rindlavwestling A, Stading M, Hermansson AM, Gatenholm P (1998) Structure mechanical and barrier properties of amylose and amylopectin films. Carbohydr Polym 36(2–3):217–224
25. Cano A, Jiménez A, Cháfer M, Gónzalez C, Chiralt A (2014) Effect of amylose: amylopectin ratio and rice bran addition on starch films properties. Carbohydr Polym 111:543–555
26. Liu Y, Xu J, Gao X, Sun Y, Lv JJ, Shen S, Wang S (2017) Freestanding transparent metallic network based ultrathin foldable and designable supercapacitors. Energy Environ Sci 10(12):2534–2543
27. Peng Q, Li S, Han B, Rong Q, Lu X, Wang Q et al (2016) Colossal figure of merit in transparent-conducting metallic ribbon networks. Adv Mater Tech 1(6)
28. Byars J, Singh M (2016) Rheological and textural properties of pulse starch gels. Starch-Stärke 68(7–8):778–784
29. Ren X, Song Y, Liu A, Zhang J, Yang P, Zhang J, An M (2015) Experimental and theoretical studies of DMH as a complexing agent for a cyanide-free gold electroplating electrolyte. RSC Adv 5(80):64997–65004
30. Han B, Pei K, Huang Y, Zhang X, Rong Q, Lin Q, Giersig M (2014) Uniform self-forming metallic network as a high-performance transparent conductive electrode. Adv Mater 26(6):873–877
31. Gupta R, Kumar A, Sadasivam S, Walia S, Kulkarni G, Fisher T, Marconnet A (2017) Microscopic evaluation of electrical and thermal conduction in random metal wire networks. ACS Appl Mater Interfaces 9(15):13703–13712
32. Rao K, Kulkarni G (2014) A highly crystalline single Au wire network as a high temperature transparent heater. Nanoscale 6(11):5645–5651
33. Kim W, Lee S, Lee DH, Park I, Bae JS, Lee T, Jeong S (2015) Cu mesh for flexible transparent conductive electrodes. Sci Rep 5:10715
34. Van De Groep J, Spinelli P, Polman A (2012) Transparent conducting silver nanowire networks. Nano Lett 12(6):3138–3144
35. Sciacca B, van de Groep J, Polman A, Garnett E (2016) Solution-grown silver nanowire ordered arrays as transparent electrodes. Adv Mater 28(5):905–909

36. Jang H, Park Y, Chen X, Das T, Kim M, Ahn J (2016) Graphene-based flexible and stretchable electronics. Adv Mater 28(22):4184–4202
37. Hecht D, Hu L, Irvin G (2011) Emerging transparent electrodes based on thin films of carbon nanotubes graphene and metallic nanostructures. Adv Mater 23(13):1482–1513
38. Gao J, Xian Z, Zhou G, Liu JM, Kempa K (2017) Nature-inspired metallic networks for transparent electrodes. Adv Funct Mater:1705023
39. Ceseracciu L, Heredia-Guerrero J, Dante S, Athanassiou A, Bayer I (2015) Robust and biodegradable elastomers based on corn starch and polydimethylsiloxane (PDMS). ACS Appl Mater Interfaces 7(6):3742–3753
40. Laguna M, Bohn S, Jagla E (2008) The role of elastic stresses on leaf venation morphogenesis. PLoS Comput Biol 4(4):1000055
41. Fan J, Yeo W, Su Y, Hattori Y, Lee W, Jung S, Bajema M (2014) Fractal design concepts for stretchable electronics. Nat Commun 5:3266
42. Huang Q, Shen W, Fang X, Chen G, Yang Y, Huang J, Song W (2015) Highly thermostable flexible transparent and conductive films on polyimide substrate with an AZO/AgNW/AZO structure. ACS Appl Mater Interfaces 7(7):4299–4305
43. Mannsfeld S, Tee B, Stoltenberg R, Chen C, Barman S, Muir B, Bao Z (2010) Highly sensitive flexible pressure sensors with microstructured rubber dielectric layers. Nat Mater 9(10):859
44. Li T, Luo H, Qin L, Wang X, Xiong Z, Ding H, Zhang T (2016) Flexible capacitive tactile sensor based on micropatterned dielectric layer. Small 12(36):5042–5048
45. Hu X, Huang Z, Zhou X, Li P, Wang Y, Huang Z et al (2017) Wearable large-scale perovskite solar-power source via nanocellular scaffold. Adv Mater 29(42):1703236
46. Kim S, Jung S, Yoon I, Lee C, Oh Y, Hong J (2018) Ultrastretchable Conductor Fabricated on Skin-Like Hydrogel–Elastomer Hybrid Substrates for Skin Electronics. Adv Mater 30(26):1800109
47. Li R, Si Y, Zhu Z, Guo Y, Zhang Y, Pan N, et al (2017) Wearable sensors: supercapacitive iontronic nanofabric sensing (adv, mater, 36/2017) Adv Mater 29(36):1700253
48. Joo Y, Byun J, Seong N, Ha J, Kim H, Kim S, Hong Y (2015) Silver nanowire-embedded PDMS with a multiscale structure for a highly sensitive and robust flexible pressure sensor. Nanoscale 7(14):6208–6215
49. Gu Y, Wang X, Gu W, Wu Y, Li T, Zhang T (2017) Flexible electronic eardrum. Nano Res 10(8):2683–2691
50. Zhu H, Wang X, Liang J, Lv H, Tong H, Ma L, Liu Z (2017) Versatile electronic skins for motion detection of joints enabled by aligned few-walled carbon nanotubes in flexible polymer composites. Adv Funct Mater 27(21):1606604
51. BCK T, Chortos A, Dunn RR, Schwartz G, Eason E, Bao Z (2015) Tunable flexible pressure sensors using microstructured elastomer geometries for intuitive electronics. Adv Funct Mater 24(34):5427–5434
52. Kim K, Jang N, Ha S, Cho J, Kim JM (2018) Highly sensitive and stretchable resistive strain sensors based on microstructured metal nanowire/elastomer composite films. Small 14(14):1704232